applied sciences

MDPI

Article

Self-Excited Thermoacoustic Instability Behavior of a Hedge Premixed Combustion System with an Asymmetric Air/Fuel Supply or Combustion Condition

Yongbo Du [1], Yuanhang Zhang [2], Xiaojin Li [3], Jingkun Zhang [1], Yaodong Da [4,*], Yun Jia [3] and Defu Che [1]

[1] State Key Laboratory of Multiphase Flow in Power Engineering, School of Energy and Power Engineering, Xi'an Jiaotong University, Xi'an 710049, China; ybdu_boilerynwa@xjtu.edu.cn (Y.D.); zjk174865@stu.xjtu.edu.cn (J.Z.); dfche@mail.xjtu.edu.cn (D.C.)
[2] Shanghai Nuclear Engineering Research & Design Institute Co., Ltd., Shanghai 200233, China; xjtuyhzhang@163.com
[3] Yulin Hydrocarbon Research Institute Co., Ltd., Yulin 719000, China; lixiaojin0529@163.com (X.L.); yunjiahello@126.com (Y.J.)
[4] China Special Equipment Inspection and Research Institute, Beijing 100029, China
* Correspondence: dayaodong@csei.org.cn

Abstract: Self-excited thermoacoustic instability (SETAI) is an undesirable and dangerous phenomenon in combustion systems. However, its control is difficult, thus greatly limiting the development of combustion technology. Our previous works clarified how the premixed chamber length (L_P) and equivalence ratio (φ) influence SETAI behavior in a symmetrical hedge premixed combustion system. On real-world sites, however, the supply structure or combustion condition in a multi-flame system could be asymmetric due to space limitations or combustion adjustment needs. This paper aims to clarify the SETAI behavior of a combustion system with an asymmetric supply structure or an asymmetric combustion condition. The results indicate that the sound pressure amplitude under strong oscillation can reach 160 dB, which is about 5% of the total pressure. The SETAI state under the asymmetric condition is determined by the coupling between the heat release oscillation and sound pressure oscillation on each side and their cooperation. The asymmetric supply structure leads to asynchronous heat release oscillations between the two sides; it may be that one promotes oscillation and that the other suppresses it, or that both have a promotion effect but with asynchronous action, thus partly canceling each other out to lower the system's oscillation intensity. This brings an advantage for controlling SETAI, which can be achieved by only changing one side of the structure. The oscillation amplitude can be reduced by 80–90% by appropriately changing one L_P only by ~20%. Under an asymmetric combustion condition with φ differing between the two sides, the heat release oscillation on each side is dependent on the local φ but not the global φ. Consequently, SETAI can also be controlled by changing the distribution but maintaining a constant fuel feeding rate and φ. The concepts identified in this paper demonstrate that SETAI can be effectively controlled by adopting an asymmetric φ distribution or an asymmetric structure of the supply system. This provides a convenient SETAI control approach without affecting the equipment's thermal performance.

Keywords: thermoacoustic instability; acoustic waveform; asymmetric condition; supply structure; combustion equivalence ratio

check for updates

Citation: Du, Y.; Zhang, Y.; Li, X.; Zhang, J.; Da, Y.; Jia, Y.; Che, D. Self-Excited Thermoacoustic Instability Behavior of a Hedge Premixed Combustion System with an Asymmetric Air/Fuel Supply or Combustion Condition. *Appl. Sci.* **2023**, *13*, 11463. https://doi.org/10.3390/app132011463

Academic Editors: Jun Cong Ge and Jun Hee Song

Received: 11 September 2023
Revised: 10 October 2023
Accepted: 13 October 2023
Published: 19 October 2023

Copyright: © 2023 by the authors. Licensee MDPI, Basel, Switzerland. This article is an open access article distributed under the terms and conditions of the Creative Commons Attribution (CC BY) license (https://creativecommons.org/licenses/by/4.0/).

1. Introduction

Self-excited thermoacoustic instability (SETAI) is a very undesirable phenomenon for gas- and liquid-fired equipment [1–3]. The accompanying strong vibration causes large noise, equipment damage, failure, and even personal safety accidents [4]. SETAI is more likely to occur in high-intensity combustion systems, where the released heat cannot be transferred away immediately, such as gas turbines, aero-engines, low-nitrogen boilers, and even compact gas water heaters.

While SETAI has been investigated for more than 200 years, this tough problem is still the main challenge limiting the development of combustion technology in practice. The famous Rayleigh criterion [5] proposed that the coupling between pressure oscillation and reaction heat release oscillation is the main cause of SETAI, and this coupling will encourage SETAI if the phase difference is less than 90°. This criterion has been widely confirmed and acknowledged by various scholars [1,2,6–8]. However, the oscillation phase difference is very microscopic, and it is virtually impossible to use operation parameters for SETAI prediction via the Rayleigh criterion.

SETAI behavior has been proven to be affected by the equipment's structure and operation parameters, which provided the chance for SETAI control, but conflicting results have been observed with regard to the effect of the heat output [9–11], equivalent ratio (φ) [12–14], and system structure [15–18]. Due to insufficient knowledge, SETAI control is generally achieved via empirical or semi-empirical methods, mainly classified into two kinds of approaches. One is to increase the system's acoustic damping [3,15,19,20], such as by adding quarter-wave tubes, half-wave tubes, Helmholtz resonators, perforated plates, and perforated liners. The other is to affect the coupling between the sound pressure oscillation and heat release oscillation to obtain an out-of-step oscillation by changing the combustion parameters or structure dimensions [4,9,11,13,20,21], or by adopting a flow jet [15,22,23]. These detailed control strategies always require a number of costly tentative retrofits of the combustion system, which also influence the combustion or thermal performance of the equipment. More unfortunately, when the operation condition is changed, the verified control approach could become invalid.

To accurately and conveniently control SETAI, it is necessary to clarify the mechanism by which the phase relation between the sound pressure oscillation and reaction heat release oscillation is affected during combustion. Fully relating this phase difference to the operation parameters and structure dimensions is the key to solving this tough problem. Our previous work demonstrated that the premixed supply duct length (L_P), fuel flow rate (V_F), and φ have a coupled effect that allows for the identification of the phase difference between pressure and heat release oscillation [24,25] by introducing the flow rate oscillation at the combustion chamber inlet. This flow rate oscillation is caused by the pressure oscillation, and their phase difference [8] is determined by the sound pressure mode shape within the premixed duct [2], which is further collaboratively influenced by L_P and V_F. However, this flow rate oscillation could cause heat release oscillation, and there is also a phase difference between them due to the time needed for the combustion reaction. Moreover, the heat release delay time relative to the flow rate oscillation (τ) [26] is mainly influenced by the combustion φ. In such a mode, these three parameters ultimately affect the coupling between sound pressure and heat release oscillation, thus determining SETAI behavior.

This mechanism has been proven by many experiments conducted on a hedge premixed combustion system with a symmetrical air/fuel supply. With that symmetrical supply structure and combustion condition, the sound pressure distribution within the two sides of the premixed chamber is identical. Therefore, the flow rate oscillation is in phase between each side; thus, the resulting thermos-acoustic coupling effect synchronously promotes or suppresses the sound pressure oscillation. On real-world sites, however, the supply system could be asymmetric due to space limitations. The total V_F or φ cannot be changed freely, as they seriously affect the system's heat output and combustion performance. In comparison, it is more feasible to change the combustion condition on each side under a constant total V_F and global φ by adopting an asymmetric combustion condition. Both the asymmetric supply structure and asymmetric combustion condition could lead the thermos-acoustic coupling to be out of step between each side, potentially changing the system's SETAI state. However, there are very limited studies about how these asymmetric conditions influence SETAI behavior in a multi-flame combustion system. As such, this paper aims to explore SETAI behavior with an asymmetric supply structure or an asymmetric

combustion condition via experiments. The influences of these asymmetric conditions are further discussed to provide theoretical guidance for controlling SETAI in practice.

2. Experimental Methodology

2.1. Experimental Systems and Measurement

The experimental system is depicted in Figure 1, whose primary components include a combustion chamber and two premixed chambers. The air was supplied by a compressor and the fuel (propane) was provided by gas cylinders. Their flow rates were regulated by mass flowmeters with a range of 5 and 50 L/min, respectively, for propane and air. The gases were mixed in the two premixed chambers and then entered into the combustion chamber after passing through a flame stabilizer. The combustion chamber was vertically placed and the two premixed chambers were arranged horizontally and connected to the combustion chamber.

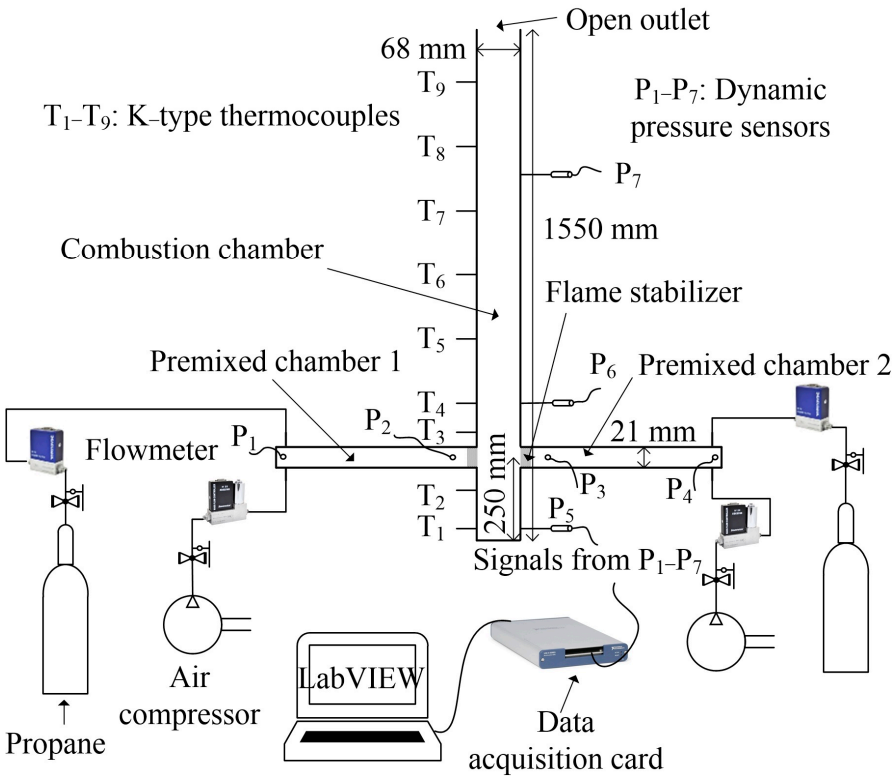

Figure 1. Schematic of the experimental setup.

The temperature distribution inside the combustion chamber was measured by placing 9 k-type thermocouples (with a maximum of 1300 K) along its vertical axis at the centerline. Seven dynamic pressure sensors (with a maximum ±10 kPa and 20 kHz for the measurement range and frequency range, respectively) were utilized to capture the pressures inside the combustion chamber and premixed chambers. During the experiment, the temperature within combustion chamber will continue to rise after ignition. After a duration of 20–30 min, the temperature field reaches a relatively steady distribution. Temperatures were manually recorded from those thermocouple indications, and the pressure signals were subsequently collected at a frequency of 10 kHz and recorded using a data acquisition system.

2.2. Data Analysis

The measured pressure variation with time (with frequency of 10 kHz) can visually illustrate the pressure oscillation conditions. In addition, the spectral analysis of these pressure signals was conducted using the Fast Fourier Transform (FFT) to identify the dominant frequency (f_M) and its amplitude of sound pressure for a quantitative analysis.

Here, the root-mean-square pressure (P_{RMS}, Pa) was used to characterize the oscillation amplitude, as given by Equation (1), and the pressure signals collected at P_5 (combustion chamber bottom) were selected for representing the oscillation behavior of system.

$$P_{\mathrm{RMS}} = \sqrt{\frac{1}{N}\sum_{i=1}^{N} {p_i}^2} \tag{1}$$

where N is the number of samples and p_i is the measured pressure.

Alternatively, the sound pressure level (SPL, dB) was also used for a broader amplitude comparison, as given in Equation (2).

$$\mathrm{SPL} = 20\lg\frac{P_{\mathrm{RMS}}/\sqrt{2}}{p_{\mathrm{ref}}} \tag{2}$$

where p_{ref} is the reference value (2×10^{-5} Pa, here).

Under sustained-oscillation conditions, a standing wave was formed within the whole system, and the mode shape is similar to a quarter wave within the combustion chamber. Consequently, the acoustic resonant frequency of combustion chamber (f) can be estimated using Equation (3), which can be used to analyze the system oscillation behavior. Here, the wave mode shape within combustion chamber is not perfectly a quarter wave, and thus f could differ slightly from the true oscillation frequency.

$$f = \frac{1}{4 \times \sum_i h_i / c_{\mathrm{mix},i}} \tag{3}$$

where h_i and $c_{\mathrm{mix},i}$ are the height and acoustic speed of the mixture gas of the ith section of the combustion chamber (divided into nine sections along height, as shown in Figure 1), respectively, and the outlet correction [27] is included in h_9.

The measured temperatures were used together with properties of mixture gas to estimate the $c_{\mathrm{mix},i}$, as shown in Equation (4).

$$c_{\mathrm{mix},i} = \sqrt{\mathrm{R}\frac{\gamma_{\mathrm{mix},i} T_i}{M_{\mathrm{mix}}}} \tag{4}$$

where M_{mix} is the molar mass of mixture (ignore the change in combustion chamber), $\gamma_{\mathrm{mix},i}$ is the adiabatic exponent of the mixture in the ith section, and T_i is the temperature measured from the ith thermocouple.

In addition, the acoustic wavelength (λ_{P}) within the premixed chamber can be calculated by the ratio of c_{mix} within the premixed chamber to the oscillation frequency (f or f_{M}). This λ_{P} is crucial for determining the pressure mode shape before the combustion chamber inlet, and thus influences the oscillation behavior through the Rayleigh criterion [24,25], as is also discussed in Section 4.1.

2.3. Set of Cases

This study primarily investigated the SETAI behavior with an asymmetric gas supply structure or under asymmetric combustion conditions. The situations under symmetrical conditions were first examined as comparison basis, as shown by the detailed experimental cases in Table 1a.

Table 1. (**a**) Cases under symmetric supply structure and combustion condition. (**b**) Cases under asymmetric air/fuel supply structure. (**c**) Cases under asymmetric supply system with two premixed chambers differing by a half wavelength. (**d**) Cases under asymmetric air/fuel supply structure and asymmetric combustion condition. (**e**) Cases under asymmetric combustion condition (L_1 = L_2 = 1.85 m).

(a)

Cases	L_P(m)	φ
1–12	0.55, 0.65, 0.86, 1.06, 1.25, 1.46, 1.65, 1.85, 2.06, 2.26, 2.46, 2.66	0.9
13–27	0.55, 0.65, 0.86, 1.06, 1.25, 1.46, 1.65, 1.85, 2.06, 2.26, 2.46, 2.66, 2.86, 3.06, 3.26	0.7

(b)

Cases	L_1(m)	L_2(m)	φ
28–38	2.06	0.55, 0.65, 0.86, 1.06, 1.25, 1.46, 1.65, 1.85, 2.26, 2.46, 2.66	0.9
39–48	1.65	0.55, 0.65, 0.86, 1.06, 1.25, 1.46, 1.85, 2.26, 2.46, 2.66	0.9
49–62	2.66	0.55, 0.65, 0.86, 1.06, 1.25, 1.46, 1.65, 1.85, 2.06, 2.26, 2.46, 2.86, 3.06, 3.26	0.7

(c)

Cases	L_1(m)	L_2(m)	φ
63	3.87	3.87	0.9
64	1.65	3.87	0.9
65	2.86	0.55	0.7

(d)

Cases	Premixed chamber 1		Premixed chamber 2	
	L_1(m)	φ_1	L_1(m)	φ_2
66	2.66	0.9	1.65	0.7
67	2.66	0.7	1.65	0.9

(e)

Cases	φ_1	φ_2
68–71	0.7	0.8, 0.9, 1.1, 1.3
72–73	0.9	1.1, 1.3

Previous work demonstrated that L_P and V_F could affect the sound pressure distributions to determine the state of SETAI, and the influence from changing L_P is more pronounced. Therefore, experiments under asymmetric gas supply structure with L_P differing on two sides were conducted, as shown by the cases in Table 1b (L_1 and L_2 represent the length of left and right premixed chamber, respectively).

In addition, previous work also demonstrated that increasing L_P by a half λ_P can result in similar oscillation conditions. With this, two additional cases were conducted to further clarify the mechanism of the asymmetric supply system influence on SETAI behavior, as shown by cases 64 and 65 in Table 1c.

On the other hand, φ also has a great impact on SETAI behavior, and thus two groups of experiments were conducted under asymmetric combustion conditions with φ differing on two sides, as shown in Table 1d,e (φ_1 and φ_2 are φ at left and right premixed chamber, respectively). All the cases in the present experiment were conducted under a constant V_F of 0.924 L/min, equally divided on both sides.

2.4. Uncertainty Analysis

In the present experiments, the measurement error of thermocouple and pressure sensor was ±50 Pa and ±6 K, respectively. The error of pressure sensor could cause an uncertainty of less than 2.5% for the oscillation amplitude under SETAI condition. Moreover, the error of thermocouple could introduce an uncertainty of 1 m/s for the sound speed, and then the resulting error for f was less than 0.5%. In addition, the measurement error of

flowmeter was ±0.0174 L/min in propane flow rate and ±0.1006 L/min for air flow rate. These errors could contribute to a maximum error of 2.8% for φ.

3. Results

3.1. Oscillation Condition under Asymmetric Supply Structure

Figure 2 presents a comparison of sound pressure oscillation between an asymmetric supply structure (case 35) and two symmetric systems (cases 8 and 9). In case 35, L_1 is the same as the premixed chamber length in case 8, and L_2 is the same as the premixed chamber length in case 9. Both the symmetric structures exhibit strong oscillation, with frequencies of 70.4 and 72.6 Hz, respectively. In case 35, the sound pressures also demonstrate a strong oscillation, with its frequency spectrum showing only one peak at 72.4 Hz, rather than two separate oscillations at 70.4 and 72.6 Hz.

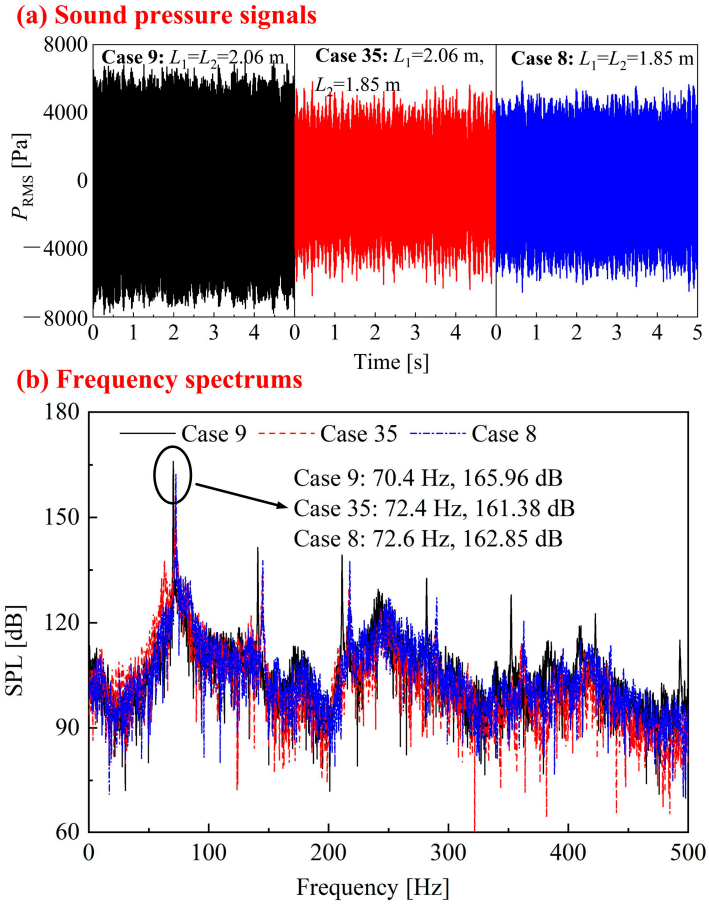

Figure 2. The pressure oscillation under asymmetric supply structure of case 35 in comparison to the two correlative symmetric supply structure (φ_1 = φ_2 = 0.9).

Figure 3 displays the oscillation characteristics of another asymmetric condition (case 32) in comparison to its corresponding symmetric systems (case 9 and 5). The frequency spectrum of case 32 exhibits a bimodal feature, similar to case 5. Additionally, an important observation is that the amplitude is lower for the asymmetric system compared to the two symmetric systems. Both Figures 2 and 3 support the notion that the sound pressure oscillation behavior of an asymmetric system does not arise from the linear superposition of the two corresponding symmetric systems, and its frequency differs from either.

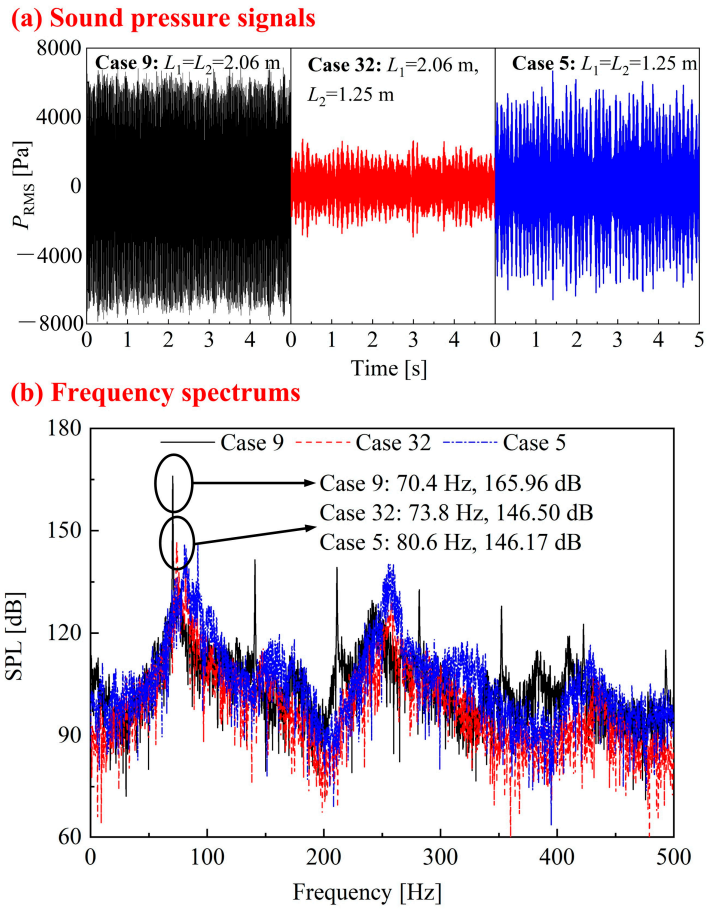

Figure 3. The pressure oscillation under asymmetric supply structure of case 32 in comparison to the two correlative symmetric systems (φ_1 = φ_2 = 0.9).

3.2. Oscillation Variation with Changing Length of One Side of Premixed Chamber

The dependence of oscillation on the length of one side of the premixed chamber was investigated while keeping the length of the other side fixed (cases 28–62 in Table 1b). The variation in sound pressure amplitude and frequency with L_2 was compared to the corresponding symmetric system (L_1 changing equally with L_2), as shown in Figures 4–6. When L_1 was fixed at 2.06 m, the combustion successively underwent non-, intermittent, and continuous oscillation as L_2 increased from 0.55 to 2.06 m. Subsequently, it returned to non-oscillation at 2.26–2.46 m, initiating another cycle. The oscillation dependence on L_2 was similar to that on L_P under the symmetric supply systems [25]. Furthermore, for all conditions of continuous oscillation, the P_{RMS} under the asymmetric supply systems was consistently lower than that of the corresponding symmetric systems. The experiments conducted under φ = 0.7 and L_1 = 2.66 m also exhibited the same trend, as shown in Figure 5. The most intense oscillation for the asymmetric supply system, with L_1 fixed at 2.06 and 1.65 m, occurred in case 35 and 45, respectively, both with L_2 = 1.85 m. The P_{RMS} values were 30% and 42% lower than those of the symmetric supply system (L_1 = L_2 = 2.06 m), respectively.

Figure 6 reveals a few minor differences compared to Figures 4 and 5. In case 45 (L_1 = 1.65 m, L_2 = 1.85 m) and case 63 (L_1 = 1.65 m, L_2 = 1.45 m), the oscillation intensity fell between those of the two corresponding symmetric systems. An intermittent oscillation occurs under case 60 (L_1 = 1.65 m, L_2 = 0.85 m), while both corresponding symmetric systems displayed sustained oscillation. The combination of 1.65 m (sustained oscillation in symmetric systems) and 2.26 m (non-oscillation in symmetric systems) resulted in sustained oscillation. These apparently irregular relationships indicate that the oscillation characteristic under asymmetric supply structures is not straightforward.

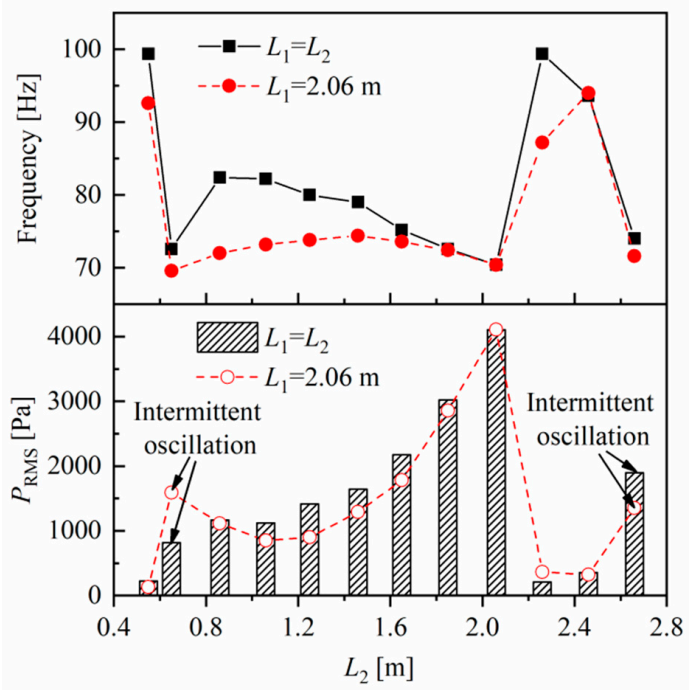

Figure 4. Oscillation variation with changing length of one side of premixed chamber in comparison to both changing equally (L_2 = 2.06 m, φ_1 = φ_2 = 0.9).

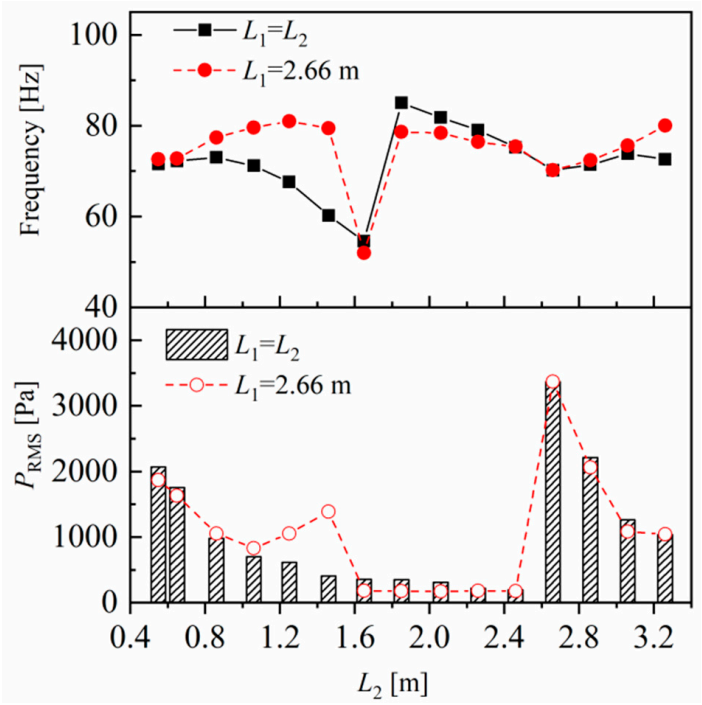

Figure 5. Oscillation variation with changing length of one side of premixed chamber in comparison to both changing equally (L_2 = 2.66 m, φ_1 = φ_2 = 0.7).

3.3. Oscillation Condition under Asymmetric Combustion Condition

Figure 7 illustrates the comparison of sound pressure oscillation and its frequency spectrum between two cases (case 66 and 67) with asymmetric supply structure and asymmetric combustion conditions. While for the supply system structure, the total V_F and global φ remain the same in both cases and case 67 exhibits strong oscillation, case 66 only

displays combustion noise. The P_{RMS} under case 66 is approximately 1/10 of that under case 67.

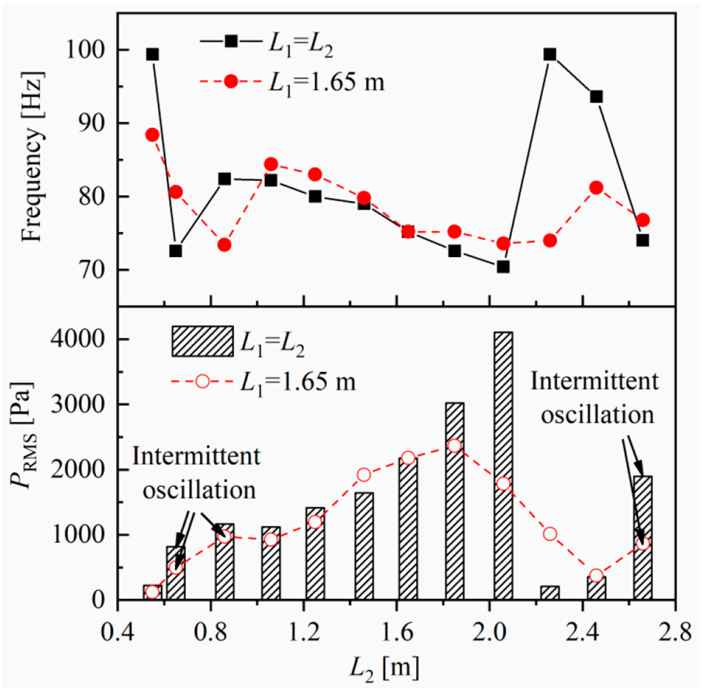

Figure 6. Oscillation variation with changing length of one side of premixed chamber in comparison to both changing equally (L_2 = 1.65 m, φ_1 = φ_2 = 0.9).

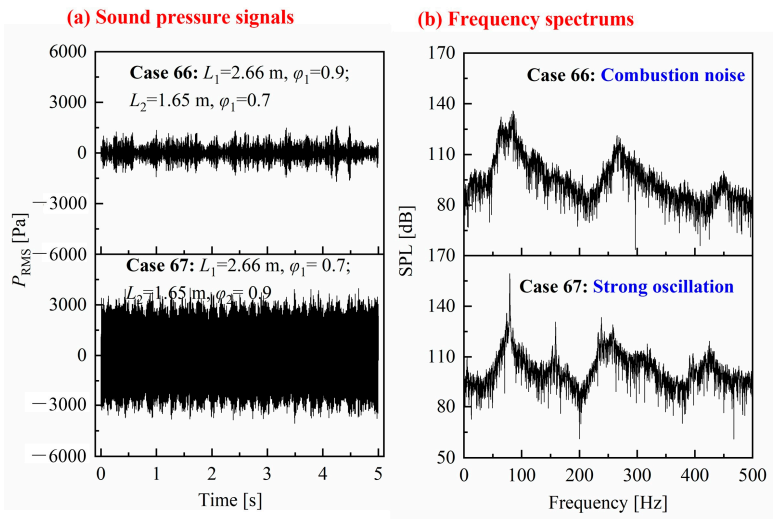

Figure 7. The pressure oscillation under asymmetric combustion condition.

4. Discussion

4.1. SETAI Behavior under Asymmetric Supply Structure

Previous investigations have shown that L_P and φ collectively influence the interaction between sound pressure oscillation and heat release oscillation, determining whether SETAI can be encouraged [9,25]. Specifically, when L_P/λ_P complies with Equation (5), the mode shape within the premixed chamber corresponds to a quarter to a half wave. In this scenario, a pressure node will exist upstream of the flame stabilizer, as the far end (inlet) of the premixed chamber acts as a pressure antinode due to its near-closed acoustic boundary condition. It should be noted that there is a potential error regarding the far end of the premixed duct not completely adhering to a closed boundary condition. Thus, when

the instantaneous pressure at the flame stabilizer exceeds its average value, the pressure will increase in the flow direction. This pressure difference between the two sides of the flame stabilizer will reduce the mixture flow rate, causing a flow rate oscillation that is phase-led by 90° relative to the pressure oscillation. In contrast, the flow rate oscillation will be phase-lagged by 90° relative to the pressure oscillation when Equation (6) is satisfied. For combustion with $\varphi = 0.9$, τ satisfies Equation (7) (where T_M is the oscillation period). This indicates that the phase lag of heat release oscillation is less than 180° relative to the flow rate oscillation. In this case, the phase difference between sound pressure oscillation and heat release oscillation would be less than 90°, promoting the oscillation as long as Equation (5) is also satisfied. When Equations (6) and (7) are simultaneously satisfied, however, the sound pressure oscillation and heat release oscillation are out of phase, resulting in a negative Rayleigh criterion that suppresses oscillation. In the combustion of $\varphi = 0.7$, however, Equation (8) is satisfied, and therefore the condition of L_P/λ_P satisfying Equation (6) can result in an oscillation promotion, while Equation (5) results in oscillation suppression. In a symmetric supply structure, both sides have the same effect of either promoting or suppressing oscillation. In an asymmetric supply system, a different L_P value may lead to the interaction between heat release oscillation and sound pressure oscillation promoting each other on one side but suppressing each other on the other side.

$$\frac{2n+1}{4} < \frac{L_P}{\lambda_P} < \frac{2n+2}{4} \tag{5}$$

$$\frac{2n}{4} < \frac{L_P}{\lambda_P} < \frac{2n+1}{4} \tag{6}$$

$$\frac{2mT_M}{2} < \tau < \frac{(2m+1)T_M}{2} \tag{7}$$

$$\frac{(2m+1)T_M}{2} < \tau < \frac{(2m+2)T_M}{2} \tag{8}$$

The ratio of L_P to λ_P was calculated on each side to analyze the mechanism of encouraging or suppressing oscillation under an asymmetric supply structure, combining the results with those obtained from measuring P_{RMS}, as shown in Tables 2–4. In asymmetric supply systems, the heat release oscillation is probably in a different phase between the two sides, generating two sources (OS_1 and OS_2, respectively) with different effects on pressure oscillation. Taking the results in Table 2 as an example, in the symmetric supply system with $L_1 = L_2 = 2.06$ m, L_P/λ_P is 0.439. Under this condition, both OS_1 and OS_2 promote oscillation, resulting in a strong oscillation with P_{RMS} as high as 4108 Pa. However, when L_2 is changed, OS_2 may suppress the oscillation, as observed in cases 29, 30, 31, and 38, resulting in an overall weak oscillation. Furthermore, it is notable that although OS_1 still has a strong promotion effect in cases 28, 36, and 37, these conditions only exhibit combustion noise without obvious oscillation.

Table 2. Ratio of L_P to λ_P on each side and the P_{RMS} ($L_1 = 2.06$ m, $\varphi_1 = \varphi_2 = 0.9$).

Case	f_M (Hz)	Premixed Chamber 1		Premixed Chamber 2			P_{RMS} (Pa)
		L_1/λ_P	Effects on Oscillation	L_2 (m)	L_2/λ_P	Effects on Oscillation	
28	91.4	0.570	Suppression	0.55	0.152	Suppression	146
29	69.6	0.434	Promotion	0.65	0.137	Suppression	1591
30	72.0	0.449	Promotion	0.86	0.187	Suppression	1112
31	73.2	0.456	Promotion	1.06	0.235	Suppression	848
32	73.8	0.460	Promotion	1.25	0.279	Promotion	899
33	74.4	0.464	Promotion	1.46	0.329	Promotion	1289
34	73.6	0.459	Promotion	1.65	0.368	Promotion	1780
35	72.4	0.451	Promotion	1.85	0.405	Promotion	2857
36	87.2	0.544	Suppression	2.26	0.596	Suppression	362
37	94.0	0.586	Suppression	2.46	0.700	Suppression	324
38	71.6	0.446	Promotion	2.66	0.576	Suppression	1352
9 (Symmetric)	70.4	0.439	Promotion	2.06	0.439	Promotion	4108

Table 3. Ratio of L_P to λ_P on each side and the P_{RMS} (L_1 = 1.65 m, $\varphi_1 = \varphi_2 = 0.9$).

Case	f_M (Hz)	Premixed Chamber 1		Premixed Chamber 2			P_{RMS} (Pa)
		L_1/λ_P	Effects on Oscillation	L_2 (m)	L_2/λ_P	Effects on Oscillation	
39	88.4	0.441	Promotion	0.55	0.147	Suppression	123
40	80.6	0.403	Promotion	0.65	0.159	Suppression	597
41	73.4	0.367	Promotion	0.86	0.191	Suppression	972
42	74.2	0.371	Promotion	1.06	0.238	Suppression	927
43	83.0	0.414	Promotion	1.25	0.314	Promotion	1194
44	79.8	0.399	Promotion	1.46	0.353	Promotion	1922
45	75.2	0.376	Promotion	1.85	0.421	Promotion	2366
46	74.0	0.370	Promotion	2.26	0.506	Suppression	1013
47	81.2	0.406	Promotion	2.46	0.605	Suppression	374
48	76.8	0.384	Promotion	2.66	0.618	Suppression	867
7 (Symmetric)	75.2	0.376	Promotion	1.65	0.376	Promotion	2176

Table 4. Ratio of L_P to λ_P on each side and the P_{RMS} (L_1 = 2.66 m, $\varphi_1 = \varphi_2 = 0.7$).

Case	f_M (Hz)	Premixed Chamber 1		Premixed Chamber 2			P_{RMS} (Pa)
		L_1/λ_P	Effects on Oscillation	L_2 (m)	L_2/λ_P	Effects on Oscillation	
49	72.6	0.582	Promotion	0.55	0.120	Promotion	1866
50	72.8	0.584	Promotion	0.65	0.143	Promotion	1632
51	77.2	0.619	Promotion	0.86	0.200	Promotion	1054
52	79.6	0.638	Promotion	1.06	0.254	Suppression	832
53	81.0	0.650	Promotion	1.25	0.305	Suppression	1054
54	79.4	0.637	Promotion	1.46	0.349	Suppression	1387
55	52.0	0.417	Promotion	1.65	0.259	Suppression	181
56	78.6	0.630	Promotion	1.85	0.438	Suppression	174
57	78.4	0.629	Promotion	2.06	0.487	Suppression	169
58	76.4	0.613	Promotion	2.26	0.521	Promotion	180
59	75.4	0.605	Promotion	2.46	0.559	Promotion	177
60	72.4	0.581	Promotion	2.86	0.626	Promotion	2062
61	75.6	0.606	Promotion	3.06	0.697	Promotion	1083
62	80.0	0.642	Promotion	3.26	0.786	Suppression	1042
24 (Symmetric)	70.2	0.563	Promotion	2.66	0.563	Promotion	3367

The results in Tables 3 and 4 also demonstrate the same regularity, where most cases show that the whole system can only be pushed into a strong oscillation when OS_2 has a promotion effect. An exceptional circumstance occurs in cases 58 and 59, where both OS_1 and OS_2 have a promotion effect, but the whole system does not exhibit oscillation. This may be because the sound pressure antinode is too close to the stabilizer [24], resulting in a relatively weak flow rate oscillation and muting the thermo-acoustic interaction. These observations indicate that, for an asymmetric supply structure, a necessary but not sufficient condition for strong oscillation is that both L_1 and L_2 satisfy oscillation promotion.

Table 5 lists the phase of sound pressure oscillation at seven measurement points under various cases. These data clearly demonstrate that the sound pressure differs within the two premixed chambers in an asymmetric supply structure. In particular, the pressure oscillation phase at the close end (P_2 and P_3) is very close in the symmetric supply structure but differs significantly in some asymmetric supply structure cases. This difference in pressure oscillation phase between P_2 and P_3 implies the asynchronized heat release oscillation between two inlets of the combustion chamber. In the symmetric supply system, the flow rate oscillation at the combustion chamber inlet is almost synchronous between the two sides, resulting in synchronous heat release oscillation. Therefore, the coupling between pressure and heat release oscillation is also the same between the two sides, and OS_1 and OS_2 have the same effect on the system's SETAI.

Table 5. Phase of sound pressure fluctuation at 7 measuring points (L_1 = 2.06 m, φ_1 = φ_2 = 0.9).

Case	L_2 (m)	Phase of Sound Pressure Fluctuation (°)							P_{RMS} (Pa)
		P_1	P_2	P_3	P_4	P_5	P_6	P_7	
28	0.55	174.2	−6.0	−17.7	−20.9	0	1.5	2.7	146
29	0.65	−168.8	5.6	−20.2	−22.6	0	2.5	1.9	1591
30	0.86	−171.4	4.3	−39.6	−44.7	0	1.9	1.9	1112
31	1.06	−172.8	3.5	−61.1	−72.3	0	1.6	1.8	848
32	1.25	−173.2	2.8	−47.6	−103.1	0	1.8	1.6	899
33	1.46	−174.4	1.3	35.6	−132.9	0	1.7	1.3	1289
34	1.65	−173.4	1.5	26.2	−148.0	0	2.0	1.3	1780
35	1.85	−169.8	3.5	20.2	−156.1	0	3.1	1.5	2857
36	2.26	176.0	−4.4	−7.6	169.7	0	0.7	1.9	362
37	2.46	170.9	−8.4	−29.0	141.3	0	1.0	1.7	324
38	2.66	−169.4	4.0	−3.5	174.6	0	3.5	1.9	1352
9 (Symmetric)	2.06	−162.4	9.3	17.6	−160	0	7.3	3.1	4108

For asymmetric supply systems, it is important to note that although OS_1 and OS_2 still experience the same pressure oscillation within the combustion chamber, their heat release oscillation may not be synchronized. Specifically, during certain periods within an oscillation cycle, the heat release oscillation may increase sound pressure on one side but have a reducing effect on the other side. In this case, there is a possibility that either OS_1 or OS_2 may individually encourage SETAI, but their promotional effects may partly cancel each other out. Consequently, the oscillation in an asymmetric supply system is generally weaker than in the two corresponding symmetric systems, as reflected in Tables 2–4 and Figures 4–6. The non-synchronous sound pressure oscillation between the two premixed chambers is the reason for the reduced oscillation under the asymmetric supply structure, and thus the system SETAI could potentially be controlled simply by altering the length of one premixed chamber.

Figure 8 compares the sound pressure oscillation in case 64 with the two corresponding symmetric systems. The oscillation condition in case 64 (L_1= 1.65 m and L_2 = 3.87 m) is almost the same as in the two symmetric supply structures, in terms of both frequency and amplitude. This is unlike the phenomenon observed in Figure 2 or Figure 3. Case 64 was specially designed such that one premixed chamber is longer than the other by half λ_P. This implies that the pressure mode shape at the upstream position of the flame stabilizer is the same between the two sides, despite having different L_P. Under the same combustion conditions, a synchronous heat release oscillation was obtained between OS1 and OS2, resulting in pressure oscillation behavior that is as strong as that in the corresponding symmetric system. The same results were observed under the condition of φ = 0.7, as shown in Figure 9.

The oscillation mechanism of these two cases was further investigated by analyzing the corresponding L_P/λ_P and the sound pressure oscillation phase at each measurement point, as shown in Tables 6 and 7, respectively. In each case, both OS_1 and OS_2 satisfy the requirements for prompting oscillation. Furthermore, what is significant is that the sound pressure oscillation is almost identical between P_2 and P_3, indicating an in-phase waveform of sound pressure that drives a synchronous flow rate oscillation between the two sides. With this and the same φ, the pressure oscillation promotion from OS_1 and OS_2 is synchronous, and hence their combined result is the same as that of the symmetric supply system. This further confirms that the system oscillation characteristic is determined by the effects on each side and their cooperation. The opposite phase between P_1 and P_4 is attributed to an additional half wave formed within the longer premixed chamber [18].

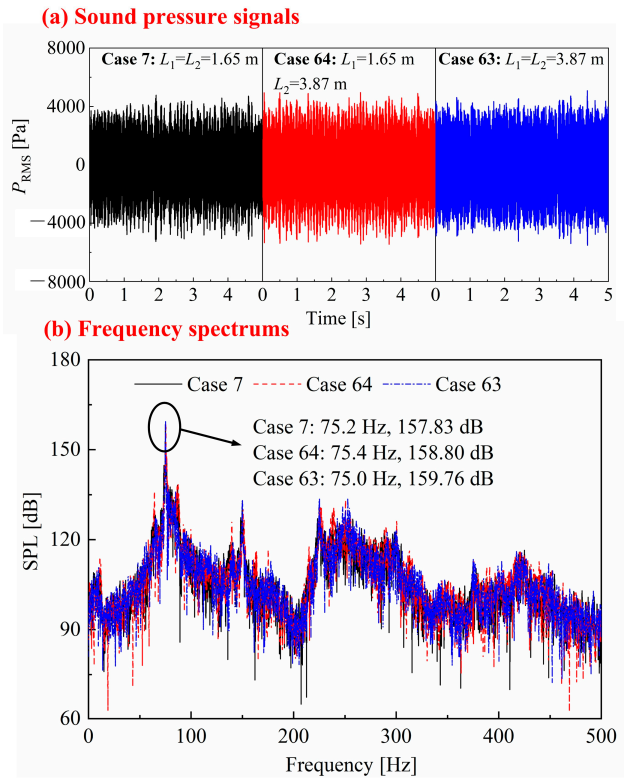

Figure 8. The pressure oscillation under asymmetric supply system of case 64 (L_1 = 1.65 m, L_2 = 3.87 m) in comparison to the two correlative symmetric systems (φ_1 = φ_2 = 0.9).

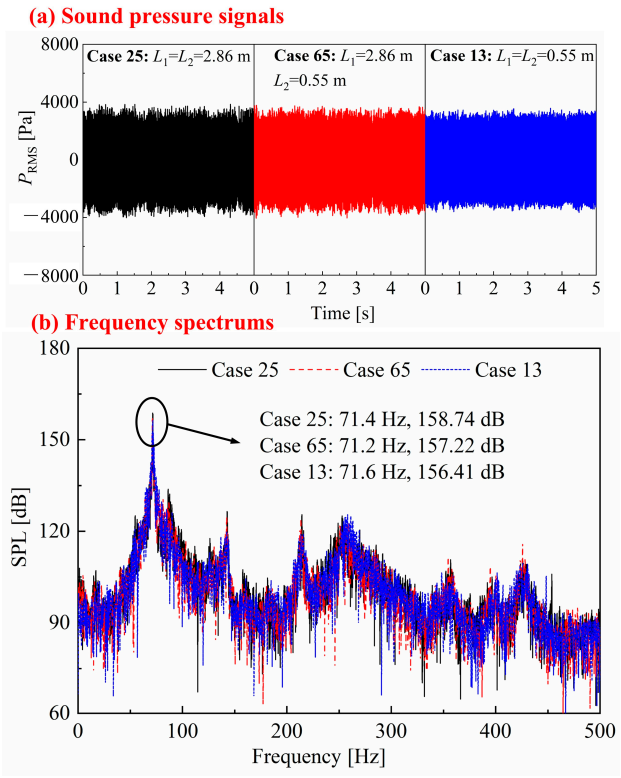

Figure 9. The pressure oscillation under asymmetric supply system of case 64 (L_1 = 2.86 m, L_2 = 0.55 m) in comparison to the two correlative symmetric systems (φ_1 = φ_2 = 0.7).

Table 6. Ratio of L_P to λ_P on each side and the P_{RMS} under cases 64 and 65.

Case	$\varphi_1 = \varphi_2$	f_M (Hz)	Premixed Chamber 1		Premixed Chamber 2		P_{RMS} (Pa)
			L_1/λ_P	Effects on Oscillation	L_2/λ_P	Effects on Oscillation	
64	0.9	75.4	0.377	Promotion	0.883	Promotion	2145
65	0.7	71.2	0.616	Promotion	0.118	Promotion	2198

Table 7. Phase of sound pressure fluctuation at 7 measuring points under case 64 and 65.

Case	Phase of Sound Pressure Fluctuation (°)							P_{RMS} (Pa)
	P_1	P_2	P_3	P_4	P_5	P_6	P_7	
64	−147.5	24.0	25.0	35.0	0.0	3.1	1.6	2145
65	162.2	−17.6	−18.8	−20.5	0.0	2.5	1.6	2198

4.2. SETAI Behavior under Asymmetric Combustion Condition

Table 8 presents the ratio of L_P to λ_P on each side and the measured P_{RMS} for two different asymmetric combustion conditions, namely cases 66 and 67. In case 67, both OS_1 and OS_2 promote oscillation, but neither satisfies the requirement for promoting oscillation in case 66. This observation aligns with the findings illustrated in Figure 7, and it supports the notion that the occurrence of oscillation in an asymmetric condition is not determined by the overall φ but is dependent on the specific condition (combination of L_P/λ_P and φ) on each side. Under an asymmetric combustion condition where φ varies between the two sides, the value of τ relies on the local φ, rather than the global φ. This is logical since the heat release at each flame should be controlled by the local φ, rather than being influenced by the total φ [24,26]. Consequently, the heat release oscillation differs between the two sides, even when there is an identical flow rate oscillation. This discrepancy leads to an unsynchronized effect on the pressure experienced on both sides.

Table 8. Ratio of L_P to λ_P on each side and the P_{RMS} under asymmetric combustion condition of cases 66 and 67.

Case	f_M (Hz)	Premixed Chamber 1			Premixed Chamber 2			P_{RMS} (Pa)
		L_1/λ_P	φ_1	Effects on Oscillation	L_2/λ_P	φ_1	Effects on Oscillation	
66	85.0	0.637	0.9	Suppression	0.397	0.7	Suppression	436
67	79.4	0.684	0.7	Promotion	0.423	0.9	Promotion	1947

It can be hypothesized that altering φ on each side, even with a consistent total φ, may impact the oscillation characteristic of the system, similar to adopting an asymmetric structure for air/fuel supply. To validate this hypothesis, experiments were conducted under symmetric supply structures ($L_1 = L_2 = 1.85$ m) but with asymmetric combustion conditions, as detailed in Table 1e. Figure 10 illustrates the observed oscillation characteristic, while Table 9 analyzes the respective effects of OS_1 and OS_2. Previous experiments have demonstrated that a φ range of 0.7–0.8 and 0.9–1.4, respectively, needs to be combined with an L_p/λ_P range of $(2n/4, (2n + 1)/4)$ and $(n/4, 2n/4)$ in order to generate a promotion effect. Among cases 68–73, where L_P is 1.85 m, φ values of 0.9, 1.1, and 1.3 satisfy this requirement. Consequently, both sides have a promotion effect in cases 72 and 73, which is consistent with the observations in Figure 10 and Table 7, where strong oscillation occurs under these two cases. In cases where OS_2 promotes oscillation but OS_1 suppresses it, weak oscillation was observed in case 69, while non-oscillation occurs in cases 70 and 71.

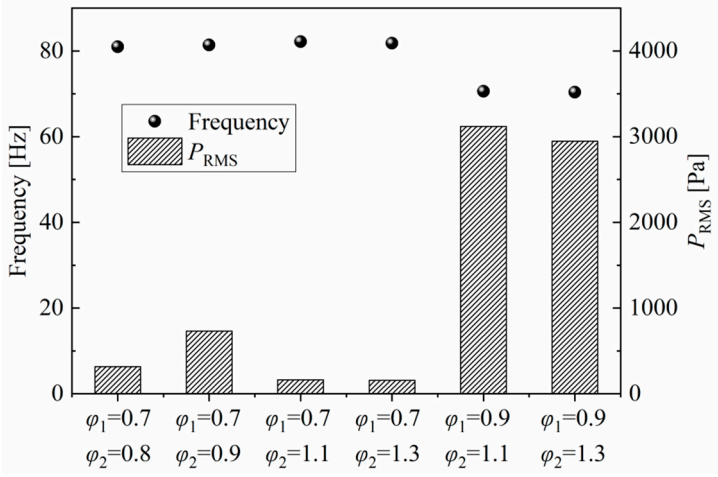

Figure 10. The pressure oscillation condition under asymmetric combustion conditions of cases 68–73.

Table 9. Ratio of L_P to λ_P on each side and the P_{RMS} under asymmetric combustion condition of case 68–73.

Case	f_M (Hz)	Premixed Chamber 1			Premixed Chamber 2			P_{RMS} (Pa)
		L_1/λ_P	φ_1	Effects on Oscillation	L_2/λ_P	φ_1	Effects on Oscillation	
68	81.0	0.452	0.7	Suppression	0.453	0.8	Suppression	316
69	81.4	0.454	0.7	Suppression	0.456	0.9	Promotion	731
70	82.2	0.458	0.7	Suppression	0.462	1.1	Promotion	163
71	81.8	0.456	0.7	Suppression	0.462	1.3	Promotion	159
72	70.6	0.395	0.9	Promotion	0.397	1.1	Promotion	3120
73	70.4	0.394	0.9	Promotion	0.397	1.3	Promotion	2947

In the case of an asymmetric supply structure with a symmetric combustion condition, τ on two sides is identical, but the sound pressure waveform is different, resulting in distinct effects on system oscillation. In comparison, the situation for an asymmetric combustion condition differs in approach but yields similar results. Consequently, SETAI can also be controlled by generating different effects through the asymmetric φ distribution between the two sides. For instance, in case 72, where the global φ is 0.91, a strong oscillation is observed under the symmetric combustion condition (φ_1 = φ_2 = 0.9) with the same supply system. In case 71, however, the asymmetric combustion condition of φ_1 = 0.7 and φ_2 = 1.3 suppresses the oscillation, without modifying the total heat release or structure. This finding holds significant importance for controlling SETAI in actual combustion systems.

5. Conclusions

This paper investigates the SETAI behavior under a hedge premixed combustion condition, focusing on the influence of the asymmetric structure of the air/fuel supply system and the asymmetric combustion condition. To achieve this, experiments were conducted with different L_P or different φ on each side. The main conclusions are as follows:

(1) The SETAI characteristic under an asymmetric condition is not simply the combination of the states under the two corresponding symmetric conditions. Instead, it is determined by the condition on each side and the cooperation between them in influencing sound pressure oscillation.

(2) An asymmetric supply structure has different effects on two sides, potentially promoting oscillation on one side while suppressing it on the other side. The system with an asymmetric supply structure can generate strong oscillation only when the coupling between heat release oscillation and sound pressure oscillation on both sides promotes oscillation. Even so, the promotion effect may be asynchronous between

the two sides, partly cancelling each other out and reducing the system's oscillation amplitude. Adopting an asymmetric supply structure allows for control of SETAI by only changing the length of one side of the premixed chamber, which is more convenient than a symmetric structure distribution.

(3) Under an asymmetric combustion condition with different φ on two sides, the oscillation of heat release on each side depends on the local φ, not the global φ. This causes different effects on two sides due to the different phase relation between heat release and sound pressure oscillation. The concepts identified in this paper demonstrate that SETAI can be effectively controlled by adopting an asymmetric φ distribution or an asymmetric structure of the supply system. This provides the potential to control SETAI without changing the fuel feeding rate, global φ, and other main combustion parameters, thus preserving the equipment's thermal performance.

Further investigation into how asynchronous heat release oscillations are coupled to influence pressure can provide a better understanding of SETAI behavior under asymmetric conditions. In addition, the dependence of SETAI behavior on the supply structure before premixing will be investigated to develop a better asynchronous control technology for SETAI in multi-flame combustion systems.

Author Contributions: Conceptualization, Y.D. (Yongbo Du) and Y.Z.; formal analysis, J.Z. and X.L.; funding acquisition, Y.D. (Yongbo Du); investigation, Y.Z., Y.J. and J.Z.; project administration, Y.J. and Y.D. (Yaodong Da); supervision, Y.D. (Yaodong Da) and D.C.; writing—original draft, Y.D. (Yongbo Du) and Y.Z.; writing—review and editing, Y.D. (Yongbo Du) and D.C. All authors have read and agreed to the published version of the manuscript.

Funding: The authors acknowledge financial support from the Shaanxi Province key research and development plan (2023-YBGY-287) and the Shaanxi Provincial Technology Innovation Guidance Special Project (2022QFY06-02), China.

Institutional Review Board Statement: Not applicable.

Informed Consent Statement: Not applicable.

Data Availability Statement: The data presented in this study are available on request from the corresponding author. The data are not publicly available, due to privacy.

Acknowledgments: The authors would like to thank Zhang, X, in the Thermal Engineering Department of Xi'an Jiaotong University for his conscientious help and work in setting up the test bench.

Conflicts of Interest: Author Yuanhang Zhang was employed by the Shanghai Nuclear Engineering Research & Desige Institute Co., Ltd.; Author Xiaojin Li was employed by the Yulin Hydrocarbon Research Institute Co., Ltd.; Author Yun Jia was employed by the Yulin Hydrocarbon Research Institute Co., Ltd.; The remaining authors declare that the research was conducted in the absence of any commercial or financial relationships that could be construed as a potential conflict of interest.

References

1. Buschmann, P.E.; Mensah, G.A.; Moeck, J.P. Intrinsic thermoacoustic modes in an annular combustion chamber. *Combust. Flame* **2020**, *214*, 251–262. [CrossRef]
2. Dang, N.; Zhang, J.; Deguchi, Y. Numerical Study on the Route of Flame-Induced Thermoacoustic Instability in a Rijke Burner. *Appl. Sci.* **2021**, *11*, 1590. [CrossRef]
3. Wang, J.; Rubini, P.; Qin, Q.; Houston, B. A Model to Predict Acoustic Resonant Frequencies of Distributed Helmholtz Resonators on Gas Turbine Engines. *Appl. Sci.* **2019**, *9*, 1419. [CrossRef]
4. Poinsot, T. Prediction and control of combustion instabilities in real engines. *Proc. Combust. Inst.* **2017**, *36*, 1–28. [CrossRef]
5. Rayleigh, L. The explanation of certain acoustical phenomena. *Nature* **1878**, *18*, 319–321. [CrossRef]
6. Fournier, G.J.J.; Haeringer, M.; Silva, C.F.; Polifke, W. Low-Order Modeling to Investigate Clusters of Intrinsic Thermoacoustic Modes in Annular Combustors. *J. Eng. Gas Turbines Power* **2021**, *143*, 041025. [CrossRef]
7. Bomberg, S.; Emmert, T.; Polifke, W. Thermal versus acoustic response of velocity sensitive premixed flames. *Proc. Combust. Inst.* **2015**, *35*, 3185–3192. [CrossRef]
8. Luo, L.; Li, T.; Deng, J.; Zhao, R.; Wang, J.; Xu, L. Experimental Investigation on Self-Excited Thermoacoustic Instability in a Rijke Tube. *Appl. Sci.* **2022**, *12*, 8046. [CrossRef]

9. Baraiya, N.A.; Ramanan, V.; Baladandayuthapani, N.; Vegad, C.S.; Chakravarthy, S.R. Investigation of Oscillatory States Involving Acoustic Mode Shifts in a Turbulent Syngas Combustion Using Non-Stationary Time-Series Analysis. *Flow Turbul. Combust.* **2021**, *107*, 1067–1089. [CrossRef]
10. Kim, M.-K.; Yoon, J.; Oh, J.; Lee, J.; Yoon, Y. An experimental study of fuel–air mixing section on unstable combustion in a dump combustor. *Appl. Therm. Eng.* **2014**, *62*, 662–670. [CrossRef]
11. Heydarlaki, R.; Aitchison, W.; Kostka, P.; Kheirkhah, S. Competing contributions of structural, acoustic, and intrinsic modes to thermoacoustic oscillations. *Combust. Sci. Technol.* **2022**, *194*, 2894–2915. [CrossRef]
12. Cadavid, Y.; Obando, J.; Vandel, A.; Cabot, G.; Amell, A. Effect of air humidity and natural gas composition on swirl burner combustion under unstable conditions. *Fuel* **2021**, *306*, 121601. [CrossRef]
13. Kim, J.H.; Kim, S.G.; Lee, K.M.; Park, J. An experimental study on thermoacoustic instabilities in syngas-air premixed impinging jet flames. *Fuel* **2019**, *257*, 115921. [CrossRef]
14. Wu, G.; Lu, Z.; Guan, Y.; Li, Y.; Ji, C.Z. Characterizing nonlinear interaction between a premixed swirling flame and acoustics: Heat-driven acoustic mode switching and triggering. *Energy* **2018**, *158*, 546–554. [CrossRef]
15. Wang, J.; Rubini, P.; Qin, Q. A Porous Media Model for the Numerical Simulation of Acoustic Attenuation by Perforated Liners in the Presence of Grazing Flows. *Appl. Sci.* **2021**, *11*, 4677. [CrossRef]
16. Zhou, H.; Tao, C. Effects of annular N_2/O_2 and CO_2/O_2 jets on combustion instabilities and NO_x emissions in lean-premixed methane flames. *Fuel* **2020**, *263*, 116709. [CrossRef]
17. Liu, T.; Li, J.; Zhu, S.; Yang, L. Determination of the heat conduction transfer function within the thermoacoustic instability limit cycle in a Rijke tube. *Appl. Therm. Eng.* **2022**, *206*, 118084. [CrossRef]
18. Biagioli, F.; Lachaux, T.; Narendran, S. Investigation of the Dynamic Response of Swirling Flows Based on LES and Experiments. *Flow Turbul. Combust.* **2014**, *93*, 521–536. [CrossRef]
19. Zalluhoglu, U.; Olgac, N. A study of Helmholtz resonators to stabilize thermoacoustically driven pressure oscillations. *J. Acoust. Soc. Am.* **2016**, *139*, 1962–1973. [CrossRef]
20. Oh, S.; Kim, J.; Kim, Y. Analysis for Combustion Instability and Stabilization Characteristics in a Swirled Premixed Combustor with a Slotted Plate. *J. Eng. Gas Turbines Power* **2018**, *140*, 091501. [CrossRef]
21. Idahosa, U.; Saha, A.; Xu, C.Y.; Basu, S. Non-premixed acoustically perturbed swirling flame dynamics. *Combust. Flame* **2010**, *157*, 1800–1814. [CrossRef]
22. Deshmukh, N.N.; Sharma, S.D. Suppression of thermo-acoustic instability using air injection in horizontal Rijke tube. *J. Energy Inst.* **2017**, *90*, 485–495. [CrossRef]
23. Tao, C.; Zhou, H. Effects of different preheated CO_2/O_2 jet in cross-flow on combustion instability and emissions in a lean-premixed combustor. *J. Energy Inst.* **2020**, *93*, 2334–2343. [CrossRef]
24. Zhang, Y.; Wang, C.A.; Liu, X.; Du, Y.; Che, D. Study on Passive Control of the Self-excited Thermoacoustic Oscillations Occurring in Combustion Systems. *Combust. Sci. Technol.* **2023**, *195*, 184–211. [CrossRef]
25. Zhang, Y.; Wang, C.; Liu, X.; Che, D. Numerical study of the self-excited thermoacoustic vibrations occurring in combustion system. *Appl. Therm. Eng.* **2019**, *160*, 113994. [CrossRef]
26. Gai, J.; Qiu, H.; Xiong, C.; Huang, Z. Experimental Investigation on the Propagation Process of Combustion Wave in the Annular Channel Filled with Acetylene-Air/Oxygen Mixture. *Flow Turbul. Combust.* **2022**, *108*, 797–817. [CrossRef]
27. Zhou, H.; You, H.; Li, G.; Cen, K. On the thermoacoustic vibration frequency of a Rijke combustor—Mathematical derivation and experimental verification. *J. Vib. Eng.* **2007**, *20*, 594–598.

Disclaimer/Publisher's Note: The statements, opinions and data contained in all publications are solely those of the individual author(s) and contributor(s) and not of MDPI and/or the editor(s). MDPI and/or the editor(s) disclaim responsibility for any injury to people or property resulting from any ideas, methods, instructions or products referred to in the content.